Quantitative Assessment of Climate Change Impacts on the Hydrology of the North Platte River Watershed, Wyoming

Anil Acharya, M.ASCE[1]; Thomas C. Piechota, M.ASCE[2]; and Glenn Tootle, M.ASCE[3]

Abstract: The impact of climate change on water resources is a major issue for regions in the world. Climate parameters such as temperature and precipitation are expected to change in the future and could significantly impact available water resources. This paper assesses long-term water availability over the North Platte River watershed, Wyoming, by utilizing the variable infiltration capacity (VIC) hydrologic model and developing streamflow projections under anthropogenic climate change conditions. Uncertainties in the scenarios of climate change and global climate models are assessed by utilizing ensemble multiple models and multiple scenarios from the World Climate Research Programme's database. The simulated streamflows are compared using an intermodel interscenario approach. Based on streamflow projections, there is a possibility of increased annual streamflow for this region through 2100, with maximum streamflow during 2085–2090. The simulated annual streamflows for future periods vary from −20 to 62% with respect to the baseline period (1971–2000). In the simulations, the wet months are getting wetter, whereas the summer months are found to be growing drier. The streamflow projections and the range of streamflow can be utilized by decision makers in future water supply and demand management study. **DOI: 10.1061/(ASCE)HE.1943-5584.0000543.** © *2012 American Society of Civil Engineers.*

CE Database subject headings: Climate change; Watersheds; Streamflow; Hydrology; Wyoming.

Author keywords: Climate; Anthropogenic activities; Variable infiltration capacity (VIC); Global climate models (GCMs); Streamflow.

Introduction

The impact of climate change on water resources is a major issue for the world. The likely impacts of climate change have been documented by various studies in different parts of the world (e.g., Bates et al. 1994; Aizen et al. 1997; Loukas et al. 2002; Jian and Shuo 2006). The major impacts are observed on the hydrological cycle and regional water availability for industry, domestic use, flood control, irrigation and agriculture, aquatic life survival, reservoir operation, and navigation. The hydrologic response due to climate change further affects the strategies and polices of water resource management. It has been identified that almost 90% of the observed changes to physical and biological systems on a global scale are much more likely due to increased warming [National Aeronautics and Space Administration (NASA) 2008]. The increasing temperature trends are attributed to increasing anthropogenic activities [Intergovernmental Panel on Climate Change (IPCC) 2007a, b], suggesting a general trend of increasing temperature (and drier conditions) in the midlatitudes.

Snowmelt runoff is a major source of water supply in the western United States. A significant decrease in mountain snowpack was noticed in the last century in these regions, which was primarily driven by increases in temperature rather than changes in precipitation (Mote et al. 2005; Hamlet et al. 2005). The increase in temperature was attributed to higher anthropogenic input of greenhouse gases (GHGs), ozone, and aerosols (Barnett et al. 2008). Several earlier studies showed the continuous climate disruption and hydroclimatic changes in the western United States in terms of declining snowpack, lower snow water content, earlier snowmelt, and a shift in spring runoff timing (e.g., Roos 1991; Dettinger and Cayan 1995; Stewart et al. 2005; Knowles et al. 2006).

Reconstructed climate data have also indicated the occurrence of very lengthy and severe droughts in the arid western United States in the past (USGS 2004; Woodhouse et al. 2006). The Colorado River Basin, which is a major source of water supply for the western United States, has experienced the worst drought in its observed historical record [Timilsena et al. 2007; Bureau of Reclamation (BOR) 2006]. As discussed in Miller et al. (2010), total water storage in the Colorado River Basin has decreased from 94 to 56% of capacity since 1999. The U.S. Department of the Interior (DOI) (2003) has reported a continuous increase in the consumptive use of water in the western part of the country to sustain urban growth. Persistent droughts have magnified the impacts of water shortages in some western areas where the water supply is already inadequate to meet water demands during normal water years (U.S. DOI 2003). This could create serious water conflicts in the future while meeting the higher water demand. In addition, decreased snowpack runoff could impact production of hydroelectric power, thereby creating adverse impacts on the power demand of California and other western states

[1]Assistant Professor, Alabama A and M Univ., Dept. of Civil and Mechanical Engineering, 4900 Meridian St. North, Huntsville, AL 35762; formerly, Dept. of Civil and Environmental Engineering, Univ. of Nevada Las Vegas, Las Vegas, NV, and Postdoctoral Research Associate, Idaho Water Center, Boise, ID. E-mail: anil.acharya@aamu.edu

[2]Associate Vice President for Interdisciplinary Research, Professor, Dept. of Civil and Environmental Engineering, Univ. of Nevada Las Vegas, 4505 S. Maryland Pkwy., Las Vegas, NV 89154 (corresponding author). E-mail: thomas.piechota@unlv.edu

[3]Assistant Professor, Dept. of Civil and Environmental Engineering, Univ. of Tennessee, Knoxville, TN 37996.

Note. This manuscript was submitted on June 9, 2011; approved on November 15, 2011; published online on November 17, 2011. Discussion period open until March 1, 2013; separate discussions must be submitted for individual papers. This paper is part of the ***Journal of Hydrologic Engineering***, Vol. 17, No. 10, October 1, 2012. © ASCE, ISSN 1084-0699/2012/10-1071-1083/$25.00.

(Hunter 2007). The trend of increasing water demand and declining snowpack could worsen the situation even more if the dominant effect of anthropogenic climate change continues.

Model simulations applying a number of global climate models (GCMs), regional climate models (RCMs), and multiple projections over the western United States have shown increasing temperatures for all future scenarios and regions; but it is difficult to predict the precipitation response for these regions (e.g., Leung and Ghan 1999; Kim et al. 2002; Coquard et al. 2004). It is, however, well established that the dry subtropics are likely to dry further and the wet higher-latitude regions are likely to get wetter in the future (Held and Sodden 2006). On the basis of the U.S. Global Change Research Program (2009), the projected change in temperature during the summer is expected to be higher than in winter for the western United States. A temperature rise of about 1.1°C was observed for the past decade with respect to average temperature during the period 1960–1979, and this is expected to increase further from 1.4 to 7.2°C by 2100 under increased future GHG conditions.

A number of GCMs and scenarios have been used by several studies to address uncertainty in climate-change-related studies (e.g., Covey et al. 2003; Beniston et al. 2007; Maurer 2007; Vicuna et al. 2007; Fowler and Ekström 2009). The use of a single GCM output is not considered the best approach because the observed changes are very likely prone to uncertainty (McGuffie et al. 1999). Because various GCMs simulate future climate with different accuracies for different climate emission scenarios, an ensemble of GCMs provides intermodel variance and a range of model response for hydrologic impacts of climate change, which may help in assessing future water resource impacts. The mean model result, which is obtained by averaging all the ensemble model simulations, is considered to provide the best comparison with observations for climatological mean fields (Lambert and Boer 2001; Coquard et al. 2004).

It has become a difficult task to assess with higher accuracy the basin hydrologic responses under changing climatic conditions and anthropogenic alterations (e.g., Villarini et al. 2009). The concept of stationary climate that has been utilized extensively in water resource planning for sustainable water resource management is considered inadequate due to a lack of inclusion of uncertainties associated with projected climate change conditions (e.g., Milly et al. 2008). Most regional hydroclimatic studies utilize the regional climate change scenarios from GCM output and hydrologic models to study the potential effects of climate change on existing water resources. Major uncertainties are associated with the scales (spatial and temporal) and development of scenarios used in hydroclimatic modeling. Higher spatial resolution better represents the complex terrain and diverse climate regimes of the western United States (Leung et al. 2004). Therefore, some recent studies have utilized higher-resolution climate data for multiple models and multiple scenarios available from the atmospheric science community in these regions. Raff et al. (2009) utilized the bias-corrected and spatially disaggregated (BCSD) temperature and precipitation data from the World Climate Research Program's (WCRP's) Coupled Model Intercomparison Project Phase 3 (CMIP3) database for 112 climate projections from 16 GCMs and 3 emission scenarios to drive the National Weather Service (NWS) River Forecasting System (RFS) hydrologic model over four basins in the American West. All basins resulted in an increased simulated maximum flood potential over time. Miller et al. (2010) developed a similar methodology and utilized the BCSD data for 112 climate projections integrated with future evapotranspiration to develop streamflow projections for three watersheds in the Colorado River headwater basins. This study resulted in an increasing and decreasing streamflow pattern for these watersheds over this century. These studies recommended further research on climate change studies in different regions.

The suitability of the use of process-based hydrologic models (such as VIC) to study the hydroclimatic impacts on water resources has already been demonstrated in the western United States (e.g., Hamlet et al. 2005; Mote et al. 2005; Pierce et al. 2008; Hidalgo et al. 2009; Wang et al. 2009). Therefore, hydrological simulations using process-based models and downscaled regional climate change scenarios at a higher spatial and temporal resolution may be helpful in producing plausible simulations of hydrological changes on a regional scale (Nijssen et al. 2001; Christenten et al. 2004; Hayhoe et al. 2004; Payne et al. 2004; Beyene et al. 2010; Jung and Chang 2011; Maurer et al. 2010; Shrestha et al. 2011). The methodology, model, and data sources as adopted in this study are documented elsewhere in similar climate-change-related studies (e.g., Christensen and Lettenmaier 2007; Miller et al. 2010).

This paper quantitatively assesses the potential effects of climate change on hydrology and water resources of the North Platte River watershed. The North Platte River watershed in Colorado and Wyoming is a region in the western United States in which temperature and precipitation are projected to change in the future (U.S. Global Change Research Program 2009). The North Platte River is a tributary of the Platte River, and the present available water resources in the Platte River Basin in Wyoming are fully allocated [Wyoming Weather Development Commission (WWDC) 2005; National Center for Atmospheric Research (NCAR) 2011]. In addition, the water demand for nearby river basins (i.e., Green River Basin, Wind River Basin) is expected to approach 100% while including the demands of future projects under moderate population growth scenarios (WWDC 2005; NCAR 2011). Under changing future climatic conditions, this is expected to further stress future water availability over the North Platte watershed. The North Platte River provides water for agriculture, energy production, and urban development in northern Colorado, southeastern Wyoming, and eastern Nevada (Shinker et al. 2010). Lawsuits file with the U.S. Supreme Court over the North Platte River and its main tributaries began in 1911 when Wyoming filed a lawsuit against Colorado regarding water distribution of the Laramie River (*Wyoming v. Colorado 1922*, amended 1957). During the Great Depression in the 1930s, severe drought led Nebraska to file a lawsuit against Wyoming regarding North Platte River water diversions. In 1945, the U.S. Supreme Court reached a decision for this lawsuit and set limitations on the North Platte River in Wyoming (*Nebraska v. Wyoming 1945*). Recently, in 2001, Nebraska filed a lawsuit against Wyoming and Colorado, which led to the Modified North Platte Decree of 2001 (Shinker et al. 2010). This decree resulted in the creation of the North Platte Decree Committee, which monitors the North Platte River and its main tributaries and ensures implementation of water-right decisions as determined by the U.S. Supreme Court, Exhibits 4 through 15 (*Nebraska v. Wyoming and Colorado 2001*).

Several previous studies carried out in the Great Plains region utilized different climate models and methodology to evaluate the hydrologic effects of climate change on available water resources (water demand) and biodiversity (e.g., Ojima et al. 1999; Easterling et al. 2001; Peterson 2003; Weiss et al. 2003; Kang and Ramirez 2007). Further research was recommended to address the current issues and competition for water needs among the various critical sectors in this region. This paper develops long-term streamflow projections under changing future climate conditions over the North Platte River watershed. This study represents a comprehensive study of the North Platte River watershed and adopts a multimodel ensemble technique and utilizes recently available

J. Hydrol. Eng. 2012.17:1071-1083.

BCSD climate data and a process-based hydrologic model to quantitatively assess hydrologic responses under anthropogenic climate change conditions. To achieve this goal, this paper utilizes the VIC model and climate inputs from the ensemble multimodel (16 GCMs), multiscenario (3), multiprojection (112) data from the WCRP's CMIP3 database. With both the VIC model and downscaled WCRP CMIP3 data at the same scale (12 km^2, daily), the hydrologic simulations are performed at the same spatial and temporal resolution.

As noted previously, the water supply is limited and subject to competition by various sectors in the North Platte River watershed. Management of diverse water demands in this semiarid region is considered more challenging under projected climate change conditions. The Wyoming Water Development Commission has initiated a Wyoming Weather Modification Pilot Program to address current issues related to water-rights conflicts in Wyoming (NCAR 2011). The weather modification (WM) program implemented winter cloud seeding to increase snowpack and streamflow within Wyoming's Green River Basin, Wind-Bighorn River Basin, and Platte River Basin. Future water demand is the driving force in the Wyoming Weather Modification Pilot Program (NCAR 2011). Separate studies are ongoing to evaluate the effects of operational WM programs. This study, relating to streamflow forecasting under anthropogenic climate change conditions, can be utilized in future water availability assessment and demands management over the watershed. Although this study adopts the combined approach documented by other academic research, the results obtained from this study, which indicates the likelihood of the risks of anthropogenic alteration of hydrologic responses, could be of great importance to water managers and stakeholders in the Platte River Basin in planning and managing water resource allocation while meeting the requirements of diverse water demands. Future water resource management alternatives could be suggested by decision makers as a proactive step in meeting the challenges of future water demands while evaluating operational water management practices (measures) over the watershed.

Methodology

Study Area

The study area is the North Platte River watershed, which lies in the states of Wyoming and Colorado at latitude 40.3125° to 41.9375° N and longitude 105.9375° to 107.0625° W (Fig. 1). The watershed contains six unimpaired streamflow gauges and eight SNOTEL stations operated by the USGS and the National Resource Conservation Service (NRCS), respectively. The annual precipitation varies from 60 to 150 cm (25 to 60 in.) with 40 to 70 % falling as winter snow (WWDC 2005). The North Platte River, which is a tributary of the Platte River and starts at the high basin of North Park in north-central Colorado, flows northward into Wyoming along the west side of Medicine Bow ranges and finally meets the Medicine Bow River and Seminoe Reservoir. The Platte River is a tributary of the Missouri River, which is a tributary of the Mississippi River.

Hydrologic Model

The hydrologic model that is used in this analysis is the VIC (Liang et al. 1994; Cherkauer and Lettenmaier 2003), which is a macroscale, physically based, semidistributed, land surface hydrologic model. The VIC model has been used in a variety of water resource applications and climate change studies (e.g., Hamlet et al. 2005; Hidalgo et al. 2009). The major input data such as meteorological

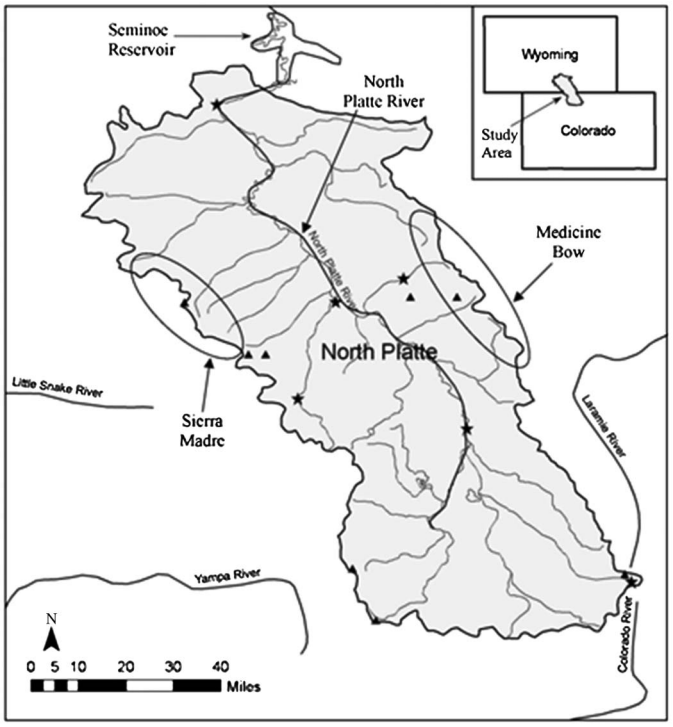

Fig. 1. Location of North Platte River, streamflow gauges (filled stars), and SNOTEL stations (filled triangles) inside North Platte River watershed

forcing data (in essence precipitation, maximum and minimum temperature, and wind speed), land cover, soil, elevation bands, and other watershed characteristics are 1/8-degree gridded data. The VIC model operates in two modes: waterbalance and energy balance; simulations are carried out at daily or subdaily time steps on the basis of these two modes of operation. The water balance mode does not solve the surface energy balance, while the energy balance mode solves the total water balance and simulates surface energy fluxes to compensate for incoming total radiation fluxes. Simulations are carried out for each grid cell, and the time series of output variables (e.g., runoff, soil moisture, evapotranspiration) are also stored separately for each specific grid. The energy fluxes such as sensible heat, latent heat, ground heat, ground heat storage, and outgoing long wave are incorporated in the energy balance mode.

A separate river routing model (Lohmann et al. 1996) and snow model are used with the VIC model. The routing model is not used in this analysis because this analysis is focused on monthly, seasonal, or annual streamflows. The snow algorithm incorporated in the VIC model solves the surface energy balance and also includes spatially distributed snow coverage and snow sublimation. All important heat and energy fluxes (e.g., sensible and latent heat, convective energy, and internal energy), snow interception, and canopy processes are incorporated in the snow model. Two layer formulations are considered: surface layer and pack layer. The thin surface layer acts as an energy exchange layer, and the pack layer acts as a reservoir to store excess snow in the surface layer. The various simulation options inside the VIC model are set in a global parameter file.

Data Description

The retrospective meteorological forcing data (precipitation in millimeters, maximum and minimum temperature in degrees

J. Hydrol. Eng. 2012.17:1071-1083.

Celsius, and wind speed in meters per second), vegetation, soil, and snow band data are obtained from the Land Surface Hydrology Research Group of the University of Washington (2012). The retrospective meteorological data represent the observed data from various sources that are utilized in this analysis for the VIC model calibration and validation. All of these data are available for 1/8-degree grid cell for the conterminous United States. The meteorological forcing data are in a binary format and daily time steps for the period 1949–2000. These data were derived (at a 3-h time step) directly from observations, with the balance of both land surface water and energy budget at each time step during hydrologic simulation (Maurer et al. 2002). The daily wind speed (meters per second) represents wind speed measured at 2 m above the ground surface. The soil parameter file contains geographical information for each grid cell and grid cell soil parameters including initial soil moisture conditions. The vegetation parameter file defines the different land cover types, the coverage in each grid cell, and other vegetation parameters (e.g., LAI-leaf area index, root depth). The snow band file contains information on each elevation band that is used by snow model.

The SNOTEL stations located within the North Platte River watershed contains historical data for daily accumulated precipitation, snow depth, snow water equivalent, and temperature (max, min, average). These station data are obtained from the National Water and Climate Center of the NRCS. They are available from the early 1980s for earlier established stations and from the early 1990s for other stations. The climate data—daily precipitation, maximum and minimum temperature—obtained from the SNOTEL stations and the GCM output are compared in this study for the period 1990–2000.

The WCRP's CMIP3 multimodel data set used in this analysis contains fine spatial resolution (1/8-degree) translations of 112 contemporary climate projections for 3 major climate emission scenarios (A1B, A2, and B1) from the IPCC and 16 robust GCMs for the contiguous United States (Maurer et al. 2007). These multiple climate projections represent the output from various GCMs, which are utilized in this analysis to derive multiple long-term streamflow projections over the North Platte River watershed. These GCMs were developed from different parts of the world, and each GCM possesses one to five projection runs for each emission scenarios as summarized in Table 1. These climate emission scenarios are considered as marker scenarios from the IPCC for future GHG emissions. They represent the projections of CO_2 emissions produced by a range of integrated assessment models based on a range of socio-economic storylines, demographic, and technological changes. The three emission scenarios are categorized as higher (A2, CO_2 concentration $\tilde{8}20$ ppm by 2100), medium (A1B, CO_2 concentration $\tilde{7}00$ ppm by 2100), and lower forcing (B1, CO_2 concentration $\tilde{5}50$ ppm by 2100) for the multimodel runs. A more detailed description of the type of GCMs and scenarios is available through the "Bias Corrected and Downscaled WCRP CMIP3 Climate Projections" archive at

Table 1. Global Climate Models (GCMs) and Abbreviated WCRP CMIP3 ID Used in This Analysis; Table also Shows the Models, Originating Group, Country, Projection Runs for Emission Scenarios, and Primary Reference

Originating group, country	WCRP CMIP3 I.D.	SRES A2 runs	SRES A1B runs	SRES B1 runs
Bjerknes Centre for Climate Research, Norway	BCCR-BCM2.0	1	1	1
Canadian Centre for Climate Modeling & Analysis, Canada	CGCM3.1 (T47)	1...5	1...5	1...5
Meteo-France/Centre National de Recherches Meteorologiques, France	CNRM-CM3	1	1	1
CSIRO Atmospheric Research, Australia	CSIRO-Mk3.0	1	1	1
U.S. Dept. of Commerce/NOAA[a]/ Geophysical Fluid Dynamics Laboratory, USA	GFDL-CM2.0	1	1	1
U.S. Dept. of Commerce/NOAA/Geophysical Fluid Dynamics Laboratory, USA	GFDL-CM2.1	1	1	1
NASA[b]/Goddard Institute for Space Studies, USA	GISS-ER	1	2, 4	1
Institute for Numerical Mathematics, Russia	INM-CM3.0	1	1	1
Institut Pierre Simon Laplace, France	IPSL-CM4	1	1	1
Center for Climate System Research (Univ. of Tokyo), National Institute for Environ. Studies, and Frontier Research Center for Global Change (JAMSTEC), Japan	MIROC3.2 (medres)	1...3	1...3	1...3
Meteorological Institute of the Univ. of Bonn, Met. Research Institute of KMA, and Model and Data Group, Germany/Korea	ECHO-G	1...3	1...3	1...3
Max Planck Institute for Meteorology, Germany	ECHAM5/MPI-OM	1...3	1...3	1...3
Meteorological Research Institute, Japan	MRI-CGCM2.3.2	1...5	1...5	1...5
National Center for Atmospheric Research, USA	CCSM3	1...4	1...3, 5...7	1...7
National Center for Atmospheric Research, USA	PCM	1...4	1...4	2...3
Hadley Center for Climate Prediction and Research/Met. Office, UK	UKMO-HadCM3	1	1	1

Note: data from http://gdo-dcp.ucllnl.org/downscaled_cmip3_projections; http://www.pcmdi.llnl.gov/ipcc/model_documentation/ipcc_model_documentation.php.

[a]National Oceanic and Atmospheric Administration.

[b]National Aeronautics and Space Administration.

http://gdo-dcp.ucllnl.org/downscaled_cmip3_projections. Since the future climate is not known exactly and all scenarios make different assumptions about future climate, all climate model outputs are considered in this analysis. All projections are treated equally likely, which provides an ensemble representation of future climate conditions.

The multimodel data set consists of statistically downscaled average monthly temperature and precipitation data from 1950 to 2100. There is a need to further temporally downscale the bias-corrected and spatially downscaled (BCSD) monthly data based on the VIC model daily input requirement. The BCSD monthly data for each grid are downscaled to daily data via random sampling and temporal downscaling (Wood et al. 2004). During random sampling, a random month is selected from historical observations that represent the same month that needs downscaling. Anomaly fields (multiplicative for precipitation and additive for temperature) are constructed with respect to observed and modeled data, which are different for each calendar month and are applied to data series to downscale it from monthly to daily time intervals. The daily wind speed (meters per second) data required for the VIC model for future climate simulations are developed by generating random samples from historical wind observations.

Model Calibration

The VIC model that is used in this analysis was calibrated for the North Platte River watershed. Calibration and validation of the model were done in the energy balance mode of operation during the periods 1950–1980 and 1981–2000, respectively, using daily meteorological forcings and historical monthly streamflow (Acharya et al. 2011). The major soil parameters such as infiltration, soil depth, base flow velocity, and soil moisture were considered for model calibration. A univariate calibration method was followed where the most sensitive soil parameters were selected and sensitivity analysis was carried out to finalize each parameter. The sensitivity analysis for each parameter was based on model performance indicators: correlation coefficient (r), root mean square error (RMSE), bias percentage, and Nash-Sutcliffe efficiency (NSCE). During calibration, the selected model parameters were varied within their minimum and maximum ranges (one parameter at a time keeping others constant), and the model performance indicators were calculated for each case. The model parameter values at which the simulation resulted in lower RMSE and bias and higher r and NSCE were finalized. The finalized calibrated parameters were infiltration parameter ($b_{\text{inf}} = 0.19$), maximum base flow ($Ds_{\text{max}} = 11$ mm/day), fraction of Ds_{max}(Ds $= 0.04$), fraction of maximum soil moisture ($Ws = 0.15$ mm/day), and soil depth ($d2 = 0.30$ m).

Model Simulations

The downscaled daily forcing data for each grid located on the North Platte River watershed and climate projection (scenario) are forced into the calibrated VIC model. A continuous simulation is carried out from 1950 to 2100 to observe the long-term streamflow projections under anthropogenic climate conditions. Model simulations are carried out for multiple projections from 16 GCMs and multiple scenarios (39 for A1B, 36 for A2, and 37 for B1). All comparisons in this analysis are based on simulated streamflows (for future and historical periods) derived using GCM output data. The simulated streamflows are compared between different time frames (2011–2040, 2041–2070, and 2071–2100) and time scales (monthly and annual) with respect to the baseline period (1971–2000). The simulated streamflows are compared to the unimpaired USGS gauge 06630000, which is located at the most downstream point of the North Platte River watershed but upstream of the Seminoe Reservoir.

The variation and distribution of simulated changes in streamflow for multimodel projections from each emission scenario are compared using box plots and projections probability density function (PDF) plots. Box plots provide a quantitative comparison of location (median) and scale (interquartile range). For this research, a box plot is used to show the variability in terms of mean, median, and quartiles of changes in streamflow. A PDF provides the relative likelihood of occurrence of a random variable. The kernel density function is used in this analysis as a nonparametric way of estimating the PDF for continuous random variables.

Goodness-of-Fit Test

A goodness-of-fit test provides a statistical measure of the existence of any significant difference in streamflow distributions between emission scenarios at different time periods. A two-sample Kolmogorov-Smirnov (KS) nonparametric test is used in this analysis to test the streamflow distributions of two data vectors. The KS Test measures the absolute maximum cumulative difference between the two distribution functions (Stephens 1970):

$$D = \max |Z1 - Z2| \tag{1}$$

where Z1 and Z2 represent data vectors for each distribution. When this test is performed, the null hypothesis assumes that the two data vectors (Z1 and Z2) are from the same continuous distribution; the alternative hypothesis is that they are from different distributions. The hypothesis is rejected if the test value, which is based on the maximum cumulative distance, exceeds a critical value on the basis of sample size.

The KS test is generally applied to independent samples; however, streamflow distribution may show temporal dependency in data series. A random permutation test is also applied in this analysis to verify the results from the KS test for streamflow distributions that show autocorrelation. This test is performed by randomly permuting each pair of streamflow data from two distributions that are holding the same time frame. The random permutation is carried out 1,000 times, and the final test value (in this case critical p value) is calculated on the basis of the distribution of test statistics obtained from each permutation. Each test statistic represents the maximum cumulative difference in between the two streamflow distributions for each random permutation.

Results

Precipitation and Temperature Patterns

On the basis of the ensemble climate projections for each scenario, the average annual temperature shows a linearly increasing trend for future periods when compared with the average annual temperature for the baseline period [Fig. 2(a)]. Higher temperatures are observed for the medium emission scenario (A1B) during the period 2041–2070, whereas maximum temperatures are observed for the higher emission scenario (A2) during the period 2071–2100. An increase of about 2°C is observed for all scenarios until 2040, which reaches a maximum at the end of the century (4°C for A1B, 5°C for A2, and 2.5°C for B1).

As shown in Fig. 2(b), the percentage change in annual precipitation with respect to the average annual precipitation from the baseline period shows both increasing and decreasing patterns with changes in magnitude for each scenario and time period.

J. Hydrol. Eng. 2012.17:1071-1083.

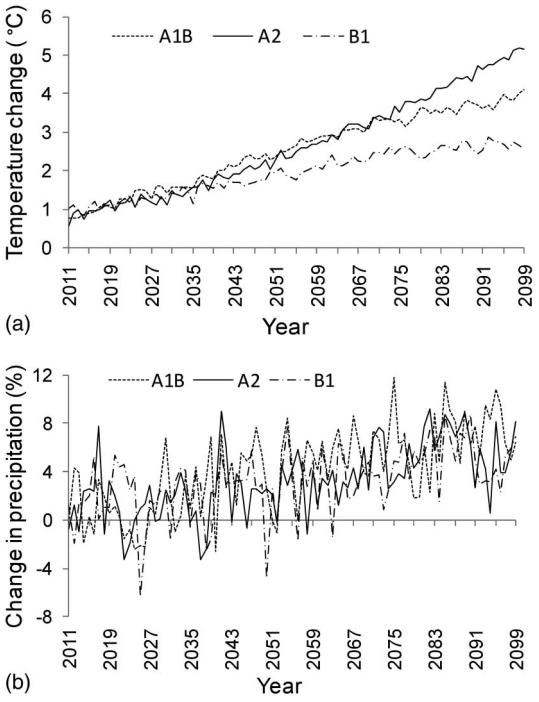

Fig. 2. Observed climate pattern for each emission scenario, averaged over multimodel climate projections from WCRP CMIP3 data set: (a) change in temperature; (b) change in precipitation, with respect to average annual temperature and precipitation for the baseline period (1971–2000)

No specific trends are observed for changing precipitation until 2035; an increasing trend is observed for scenarios at later periods—A1B after 2035, and B1 and A2 after 2050. Up to the year 2100, the calculated change in annual precipitation is between −6 and 8% for B1, between −3 and 9% for A2, and between −2 and 12% for A1B; the average increase in annual precipitation is calculated to be 3.2% for A2 and B1 and 4.2% for A1B.

The spatial distribution of modeled and observed average annual precipitation (millimeters per year) during the period 1990–1999 shows a similar distribution in most regions of the watershed [Fig. 3(a)]. Modeled precipitation from a single GCM (BCCR BCM 2.0 in Table 1) on the basis of the A1B scenario is taken here as an example for comparison. The average annual precipitation varies from 200 to 1,400 mm per year throughout the watershed, with comparatively higher precipitation toward the Colorado regions of the watershed. A good correlation is observed between the modeled and observed minimum and maximum daily temperatures for the watershed during the same period; a higher correlation is observed for the maximum temperature than the minimum temperature [Fig. 3(b)]. The modeled temperature represents the gridded average of temperatures from 112 climate projections for three emission scenarios for the watershed.

Streamflow Projections

The multimodel climate projections are forced into the calibrated VIC model to simulate streamflow projections for the watershed. The simulated annual streamflows during the period 1971–2100 for 112 climate projections from emission scenarios A1B, A2,

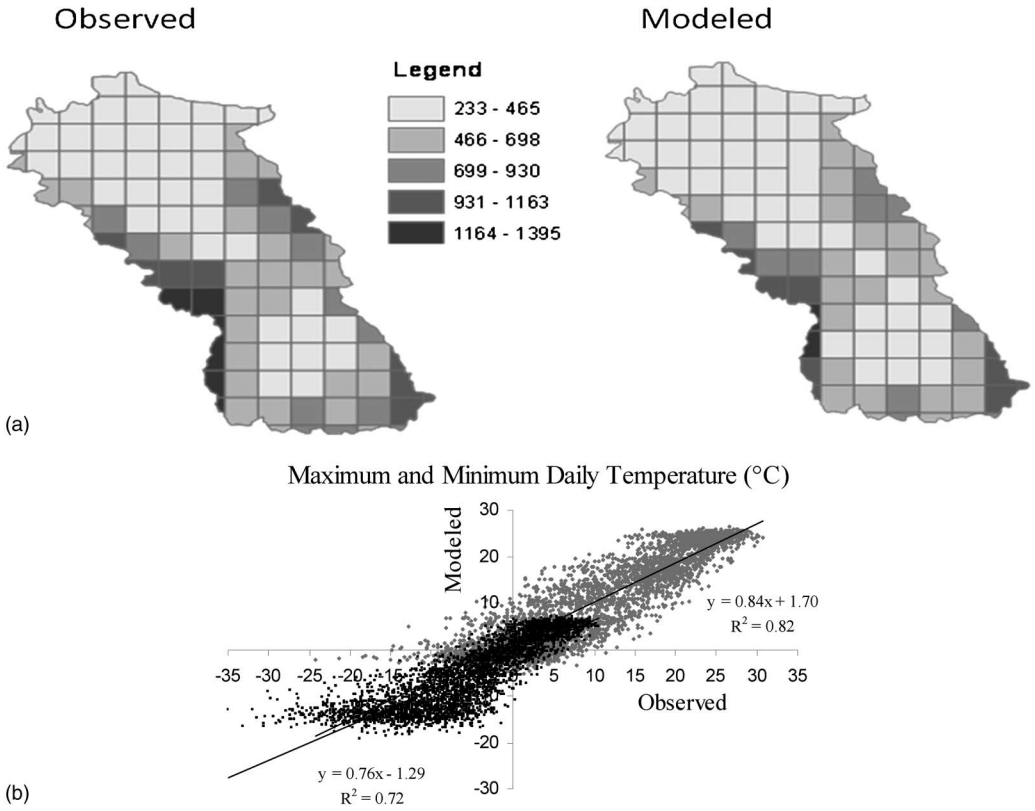

Fig. 3. (a) Spatial distribution of observed and modeled average annual precipitation (millimeters per year) for the North Platte River watershed during the period 1990–1999; (b) modeled versus observed maximum and minimum daily temperatures (°C) for North Platte River watershed during the period 1990–1999; modeled temperature represents an average temperature from 112 climate projections; light and dark gray symbols represent maximum and minimum temperatures, respectively

J. Hydrol. Eng. 2012.17:1071-1083.

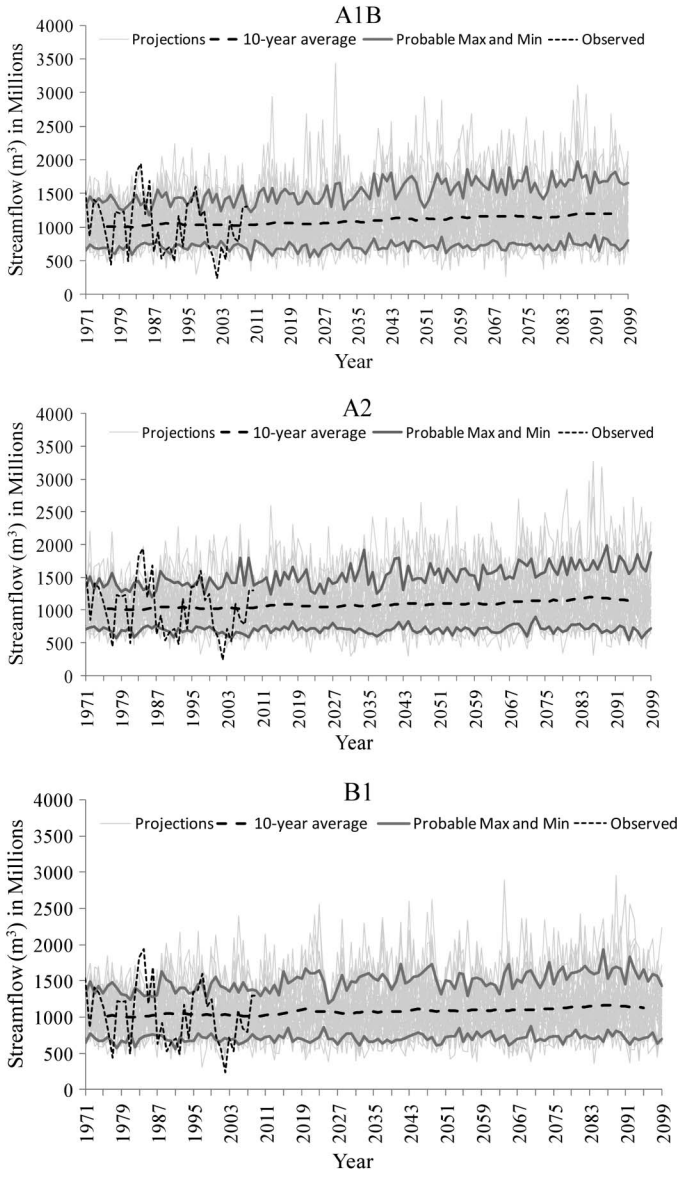

Fig. 4. Observed and model simulated long-term streamflow (cubic meters, m^3) for multimodel climate projections from emission scenarios A1B, A2, and B1, respectively; total number of climate projections: 39 for A1B, 36 for A2, and 37 for B1

and B1 are shown in Fig. 4. Maximum and minimum annual streamflows are observed at different future time periods for different climate projections. Some of the GCMs have simulated very high streamflows; the maximum annual streamflow is simulated by CCCMA CGCM 3.1.2 in the year 2030 for A1B. For probable maximum and minimum streamflows (in this case 90th and 10th percentiles) over this century, the simulated streamflows show the same range of variation between the scenarios. Both increasing and decreasing streamflow patterns are observed until the end of this century. The simulated streamflows are different between the climate projections; during certain time periods they are opposite to each other. The observed annual streamflow also shows both increasing and decreasing patterns and varies within the probable maximum and minimum range for most years (except some wet and dry years). The 10-year moving average of annual streamflow shows smaller variation as compared to the multiple projections for each emission scenario.

Interscenario Comparison

The simulated annual streamflows are compared between the scenarios. Annual streamflow represents an average of annual streamflows from all climate projections for each scenario. As shown in Fig. 5, the simulated streamflows are comparatively higher for A2 and B1 until 2020, whereas it is higher for A1B toward the end of this century. The calculated 10-year moving average shows an increasing pattern for future periods that is visible after 2020. The calculated average annual streamflows are higher during the period 2085–2090 and at their maximum in 2087 and 2089; A1B also shows a maximum annual streamflow in 2087.

The interscenario comparison of percentage change of annual streamflow with respect to average annual streamflow for the baseline period (1971–2000) is also performed. Although lower streamflows are observed for some years, the average change in streamflow indicates an increase until 2100. An average increase of about 7.2, 4.8, and 5.3% is calculated for A1B, A2, and B1, respectively, during the period 2011–2100. The calculation of percentiles, mean, minimum change, and maximum change in streamflow for all scenarios is summarized in Table 2. The mean results obtained from the ensemble multimodel climate projections are considered to address the uncertainties in the scenarios of change. Considering all scenarios, an average increase of 5.8% is calculated in annual streamflow for the projected climate change conditions.

Fig. 6 shows the average annual streamflows derived from multiple projections during the period 1971–2100 for the 90th percentile (upper solid line) and average annual streamflow (lower dotted line) for the baseline period. The number of years that exceed the 90th percentile streamflow for the baseline period increases while moving toward 2011–2040, 2041–2070, 2071–2100; all years during 2071–2100 show higher streamflows. Except for

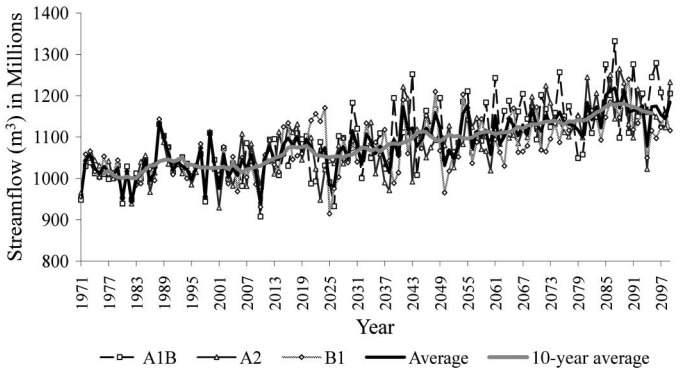

Fig. 5. Streamflow projections for emission scenarios A1B, A2, and B1 during the period 1971–2100; average streamflow represents the average of annual streamflows for all scenarios

Table 2. Calculation of Minimum, Maximum, Mean, and Percentiles of Change in Annual Streamflow (%) for Emission Scenarios A1B, A2, and B1, during the Period 2011–2100 with Respect to Baseline Period (1971–2000)

	Percentage change (%)					
Emission scenario	1st Quartile	Median	3rd Quartile	Min	Max	Mean
A1B	0.7	6.9	12.4	−12.8	27.4	7.2
A2	0.3	4.7	9.0	−10.5	23.0	4.8
B1	1.2	5.5	9.5	−13.6	22.0	5.3
Average	0.7	5.7	10.3	−12.3	24.2	5.8

J. Hydrol. Eng. 2012.17:1071-1083.

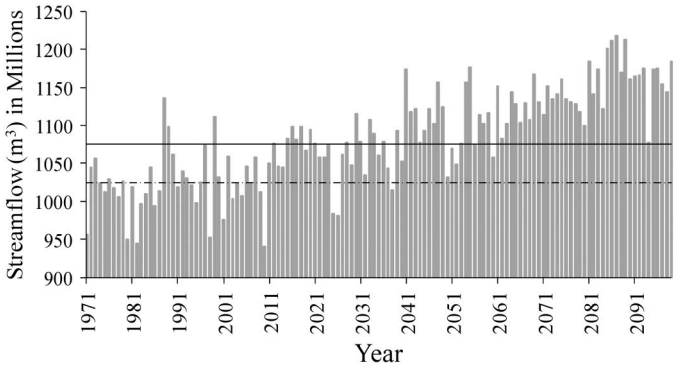

Fig. 6. Average of annual streamflows from three emission scenarios A1B, A2, and B1 during the period 1971–2100; upper solid and lower dotted lines represent 90th percentile and average annual streamflow for baseline period (1971–2000)

some years (2025–2026, 2038), all future years during the period 2011–2100 show streamflows higher than the average annual streamflow for the baseline period; a maximum decrease of 4% is calculated in annual streamflow for the years 2025/2026; a maximum increase of 19% is calculated for the year 2087.

The lower annual streamflows for some years may be due to a decrease in precipitation and a continuous increase in temperature during these periods. This causes an increase in evapotranspiration and reduction in soil moisture and streamflow. The overall increase in streamflow may be due to the projected increase in average annual precipitation and higher snow melt in a warmer future climate; an overall increase in annual precipitation with respect to average annual precipitation for the baseline period is calculated to be 3.5% for the period 2011–2100; an average increase of 5.5% is calculated for the period 2071–2100. This increasing streamflow pattern is similar to the upward trend in runoff observed for the far northwestern United States by Milly et al. (2005).

Periodical Variation

The annual streamflow for each emission scenario during 2011–2040, 2041–2070, and 2071–2100 (represented as the 2030s, 2060s, and 2090s) are compared with average annual streamflow for the baseline period. Maurer et al. (2007) suggested that the results and statements can be supported more confidently if the comparisons are made with respect to some range of time rather than a specific month or day within that time period. As shown in Fig. 7, the change in streamflow varies from −20 to 62% depending on the emission scenarios and future time periods. The highest and lowest range of variations is shown by A1B and B1, respectively. For multidecadal periods, similar increasing and decreasing streamflow patterns are observed for all scenarios; the median change in streamflow is higher during 2071–2100 and lower during 2011–2040. As noted earlier, the average annual precipitation and temperature both show a maximum increase during 2071–2100 with respect to the baseline period. An increase in precipitation and an additional runoff from snowmelt due to higher temperatures may be contributing to an increased streamflow during this period. The calculated range of median change in streamflow during 2011–2100 is higher for scenarios in the order of A1B, A2, and B1; it varies from 2 to 12%, 1 to 7%, and 4.5 to 7.5% for A1B, A2, and B1 respectively.

Nonparametric Test

The KS test is applied to monthly streamflow projections derived using 112 climate projections for various emission scenarios. Since all scenarios have the same time frame for multimodel projections, the KS test is suitable to identify if there exists any significant difference in streamflow distributions between the scenarios. The KS test rejects the null hypothesis at 5% significance level if h is 1 the p value is less than 0.05. The test statistics for all performed for this analysis are summarized in Table 3. The test statistic k measures the maximum difference observed between two cumulative streamflow distributions (1) for the same emission scenario but different periods and (2) for the same periods but different emission scenarios.

The test is first applied to streamflow projections over the period 2011–2100 with respect to the baseline period (1971–2000) separated by emission scenarios. The calculated test statistic is lower than the critical test value. Therefore, the null hypothesis that the data are coming from the same continuous distribution is rejected. This shows a significant difference in streamflow distribution over this century with the historical period streamflow for each scenario. However, an average k value of 0.18 to 0.19 for all scenarios (A1B, A2, and B1) indicates an almost equal cumulative difference in streamflow distribution if the entire future period is considered (until 2100). The combined effect of an increase in temperature for all scenarios and higher and lower precipitation patterns shown by different scenarios at different time periods during 2011–2100 (Fig. 2) may be attributed to similar changes in the total streamflow between the scenarios by the end of this century. The test is then applied to streamflow projections over the period 2011–2100 with respect to the baseline period separated by emission scenarios and multidecadal period (2011–2040, 2041–2070, 2071–2100). As expected, the null hypothesis is rejected for all cases. This indicates a significant difference between the multidecadal period and baseline period streamflow distributions within each emission scenario. Comparatively higher k values for higher emission scenarios during each multidecadal period imply that higher streamflows are simulated for A1B and A2 compared to B1, whereas

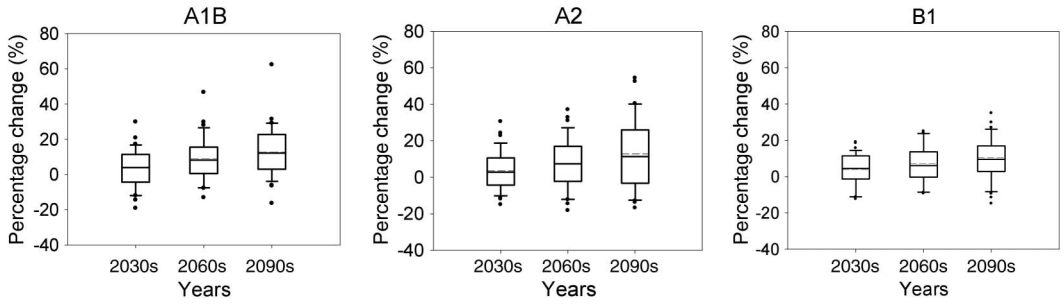

Fig. 7. Box plots of percentage change of annual streamflow for each climate emission scenario during 2011–2040, 2041–2070, and 2071–2100 (represented here as the 2030s, 2060s, and 2090s) with respect to average annual streamflow for baseline period (1971–2000)

J. Hydrol. Eng. 2012.17:1071-1083.

Table 3. Summary of Results from Two-Sample Kolmogorov-Smirnov (KS) Nonparametric Test; the k Value Is Based on Sample Size; Critical p-Values Are Calculated from KS Test as well as Random Permutation Test

Streamflow projection	Test statistic (k)	p-Value (KS test)	h	p-Value (permutation test)	Null hypothesis
A1B 2011–2100	0.18	<0.05	1	<0.05	Rejected
A1B 2011–2040	0.14	<0.05	1	<0.05	Rejected
A1B 2041–2070	0.22	<0.05	1	<0.05	Rejected
A1B 2071–2100	0.25	<0.05	1	<0.05	Rejected
A2 2011–2100	0.19	<0.05	1	<0.05	Rejected
A2 2011–2040	0.15	<0.05	1	<0.05	Rejected
A2 2041–2070	0.22	<0.05	1	<0.05	Rejected
A2 2071–2100	0.28	<0.05	1	<0.05	Rejected
B1 2011–2100	0.18	<0.05	1	<0.05	Rejected
B1 2011–2040	0.13	<0.05	1	<0.05	Rejected
B1 2041–2070	0.18	<0.05	1	<0.05	Rejected
B1 2071–2100	0.23	<0.05	1	<0.05	Rejected
A1B and A2 1971–2000	0.02	0.99	0	0.54	Accepted
A1B and A2 2011–2040	0.03	0.94	0	0.92	Accepted
A1B and A2 2041–2070	0.05	0.68	0	0.38	Accepted
A1B and A2 2071–2100	0.05	0.66	0	0.06	Accepted
A1B and A2 2011–2100	0.01	0.99	0	0.36	Accepted
A1B and B1 1971–2000	0.02	0.99	0	0.50	Accepted
A1B and B1 2011–2040	0.02	0.99	0	0.91	Accepted
A1B and B1 2041–2070	0.07	0.21	0	0.18	Accepted
A1B and B1 2071–2100	0.11	0.01	1	<0.05	Rejected
A1B and B1 2011–2100	0.04	0.08	0	0.06	Accepted
A2 and B1 1971–2000	0.03	0.99	0	0.25	Accepted
A2 and B1 2011–2040	0.03	0.99	0	0.62	Accepted
A2 and B1 2041–2070	0.05	0.62	0	0.16	Accepted
A2 and B1 2071–2100	0.16	0.01	1	<0.05	Rejected
A2 and B1 2011–2100	0.04	0.09	0	0.06	Accepted

maximum streamflows are simulated for A2 during 2071–2100. These tests demonstrate the nonstationarity nature of the future climate. A higher k value toward the end of this century for all scenarios indicates that the maximum streamflows are simulated during 2071–2100 compared to earlier periods. This could be attributed to the linearly increasing trend of temperature and precipitation toward the end of this century for all scenarios (Fig. 2).

The test is then applied to streamflow projections between the scenarios over the period 2011–2100 and for multidecadal periods. The null hypothesis is rejected only during 2071–2100 between A1B and B1, and A2 and B1. This indicates a significant difference in streamflow distributions between these scenarios. A significant increase in monthly streamflows for A1B and A2 may be due to higher temperature and precipitation for these scenarios compared with B1 during this period.

The streamflow distribution for each emission scenario shows temporal dependency in the data series with an oscillation pattern and higher autocorrelation [Fig. 8(a)]. The random permutation test is applied to all scenarios in Table 3, which results in a separate distribution of test statistic (k) for each test [Fig. 8(b)]. The bold line in Fig. 8(b) represents the location of the observed test statistic on the basis of sample size. The two streamflow distributions are considered dependent if the bold line lies inside the histogram. The critical p values for each permutation test are summarized in Table 3. The obtained results for the null hypothesis from a random permutation test is similar to the normal KS test, however, the lower p values from the permutation test demonstrates the temporal dependence of the streamflow distributions.

Intermodel Comparison

An intermodel comparison of simulated changes in streamflows for each emission scenario shows a wide range of variation when the annual streamflows for future periods (2011–2100) are compared with average annual streamflows for the baseline period. The calculated change in streamflow varies between −74 and 162% for A1B, −72 and 154% for A2, and −65 and 181% for B1 (Fig. 9).

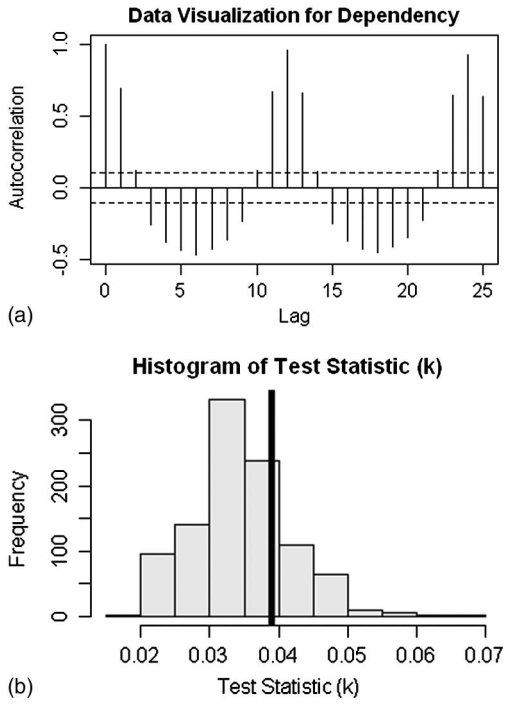

Fig. 8. (a) Autocorrelation plot of monthly streamflow from A1B scenario during 2011–2040; (b) histogram of test statistic (k) from random permutation test of monthly streamflows between A1B and A2 scenarios during 2011–2040; the middle bold line represents the k value on the basis of sample size; the two data vectors are dependent if the bold line lies inside the histogram

J. Hydrol. Eng. 2012.17:1071-1083.

The GCM that simulates the maximum change (positive or negative) also varies based on the scenario. The highest variation in annual streamflow is simulated by IPSL CM 4.1 for all scenarios; the lowest variations are simulated by miroc 3.2 medres, miub echo-g, and ncar ccsm 3 for A1B, A2, and B1, respectively. The calculated median change in streamflow is very small for some models, although they show higher variation within the model. A higher median change in streamflow is calculated for cccma cgcm3 and ncar pcm1 for all scenarios.

The distribution of percentage changes in annual streamflow for multiple models and scenarios are also compared using projection PDF plots. As displayed in Fig. 9, the PDF plot for each model shows a slight difference in its distribution patterns for different emission scenarios. For the same emission scenario, some models show changes in annual streamflow for more years compared to others. The average distribution represents an average change in annual streamflow from all model projections for each scenario. The calculated range of average distribution varies from −13 to 27% for A1B, −11 to 23% for A2, and −13 to 22% for B1. The higher concentration at zero percentage change indicates that the lower emission scenario (B1) shows changes in annual streamflow for fewer years as compared to A1B and A2; a wider distribution for A1B indicates changes in annual streamflow for more years during 2011–2100.

The diverse results in streamflow across models and scenarios, which is verified by the box plots and PDF plots of multimodel climate projections, are due to the various uncertainties resulting from climate models. These uncertainties are associated with the

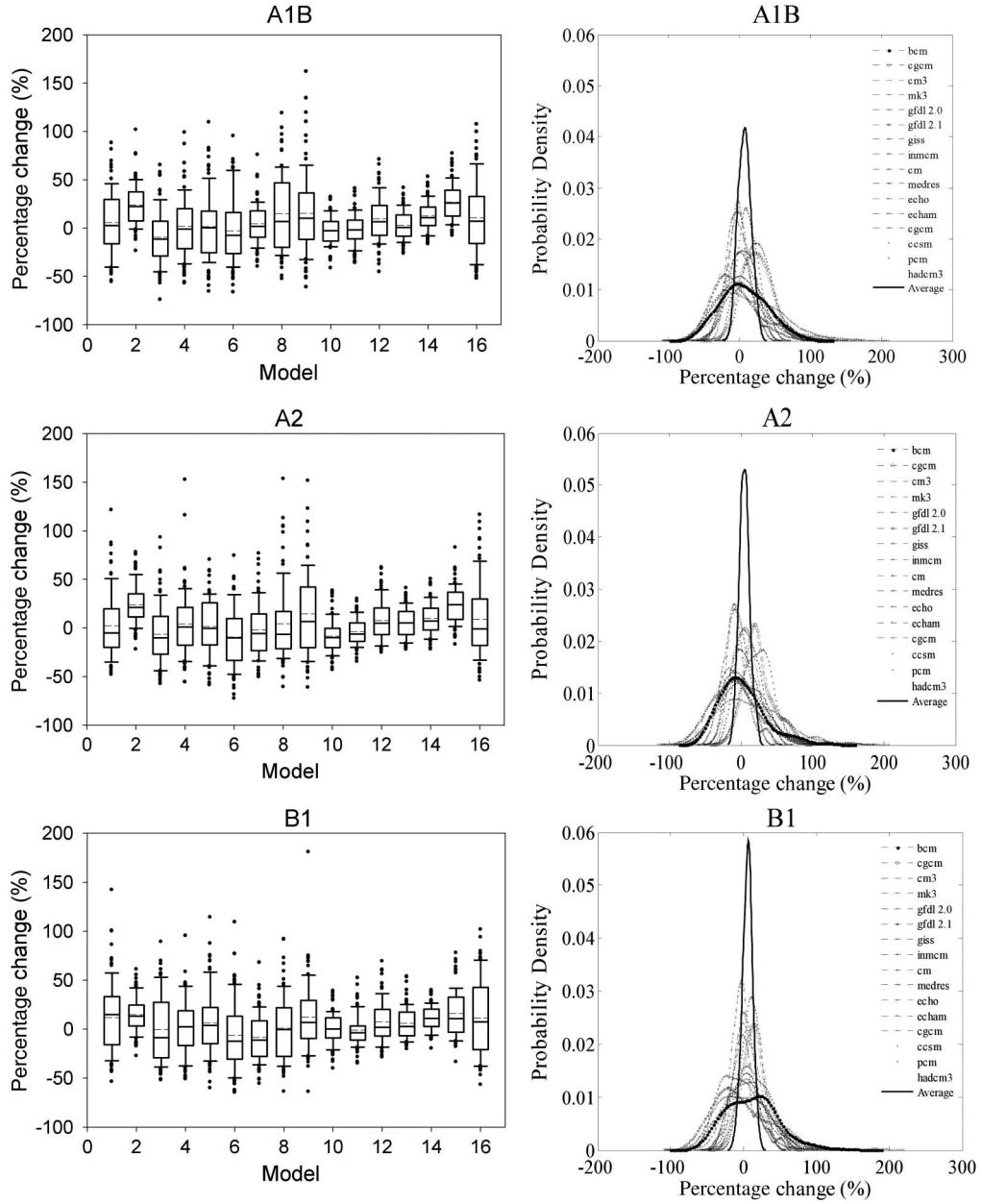

Fig. 9. Box plots and probability density function (PDF) plots for intermodel comparison of percentage change of simulated streamflows, during 2011–2100 with respect to 1971–2000, for each emission scenario. Here, 1 to 16 represents 16 global climate models used for simulation (1-bccr bcm 2.0.1; 2-cccma cgcm 3; 3-cnrm cm 3.1; 4-csiro mk 3.0.1; 5-gfdl cm 2.0; 6-gfdl cm 2.1; 7-giss model e.r.1; 8-inmcm 3.0.1; 9-ipslcm 4.1; 10-miroc 3.2 medres; 11-miub echo-g; 12-mpi echam 5; 13-mri cgcm 2.3.2a; 14-ncar ccsm 3; 15-ncar pcm 1; 16-ukmo hadcm 3.1)

J. Hydrol. Eng. 2012.17:1071-1083.

type of GCMs, emission scenarios, and climate projections. All climate projections possess different climate (meteorological) forcings for the hydrologic model simulation. The differences exist because each climate model differs in its origin, processes, physical parameterization of land surface processes, and spatial and temporal resolution (Milly et al. 2005). The model simulation capability differs based on resolution. Each model projection also possesses different assumptions for the initial and boundary conditions, GHG emissions, human-induced changes, radiation, and volcanic activity. Thus processes such as water budget and energy balance differ for different warming conditions and cause changes in the simulated streamflows.

Monthly Comparison

The monthly streamflows for each scenario during 2011–2040, 2041–2070, and 2071–2100 show larger changes in streamflow with respect to the baseline period. Monthly streamflow here represents an average of monthly streamflows from all climate projections for each scenario. As shown in Fig. 10, all scenarios show a continuous increase in streamflow for future periods during the months from October to May; a maximum increase in streamflow is observed for January and February. The summer months (June-August) show a gradual decrease in streamflow for future periods. A maximum decrease in streamflow is observed for July. In general, the simulated change (increase/decrease) is maximum for all scenarios during 2071–2100. Almost equal changes are observed in monthly streamflows for all scenarios during 2011–2040; however, the observed changes are higher for A1B and A2 during 2041–2070 and 2071–2100, respectively. An exception to this is during August when a larger decrease is observed in 2041–2070 than 2071–2100 for A1B and B1. The mean (Fig. 10) represents an average of percentage change of monthly streamflows from all scenarios. The calculated maximum decrease in monthly streamflow between the scenarios is 36%, 49 to 54%, and 55 to 61% (mean 36, 52, and 58%) during 2011–2040, 2041–2070, and 2071–2100, respectively. September shows a decrease from 2 to 4% until the end of this century. The calculated maximum increase in monthly streamflow between the scenarios varies from 74 to 77%, 148 to 195%, and 190 to 405% (mean 73%, 176%, and 308) for the same periods. On the basis of the historically observed annual streamflow, the months of April and May contribute large percentages of the total streamflow from the watershed. Therefore, the projected increases in monthly streamflow for April and May could account for the overall increases in annual streamflow.

The temperature pattern shows a warmer future climate (Fig. 2). The enhanced total precipitation with higher proportion of rainfall than snowfall, increasing soil moisture, and higher and earlier spring snowmelt due to warmer temperatures may contribute directly to a higher percentage of streamflow during what is typically the cold season. The increased warming causes a reduction in snowpack during the winter season; this reduction in mountain snowpack reduces surface albedo, which causes further reduction in winter and late spring snow cover (Leung et al. 2004). The higher snowmelt and decline of snow accumulation and the more extreme warming during the summer period increase the sensible heat, which may cause higher evapotranspiration, reduction of soil moisture, and lower streamflows. The summer months become even drier, making it difficult to meet increasing water demands. This indicates that the drier summer months will further dry and the wet months will be even wetter under anthropogenically driven climate change conditions. Similar results have been documented by Hamlet et al. (2005) in a study conducted in the Pacific Northwest.

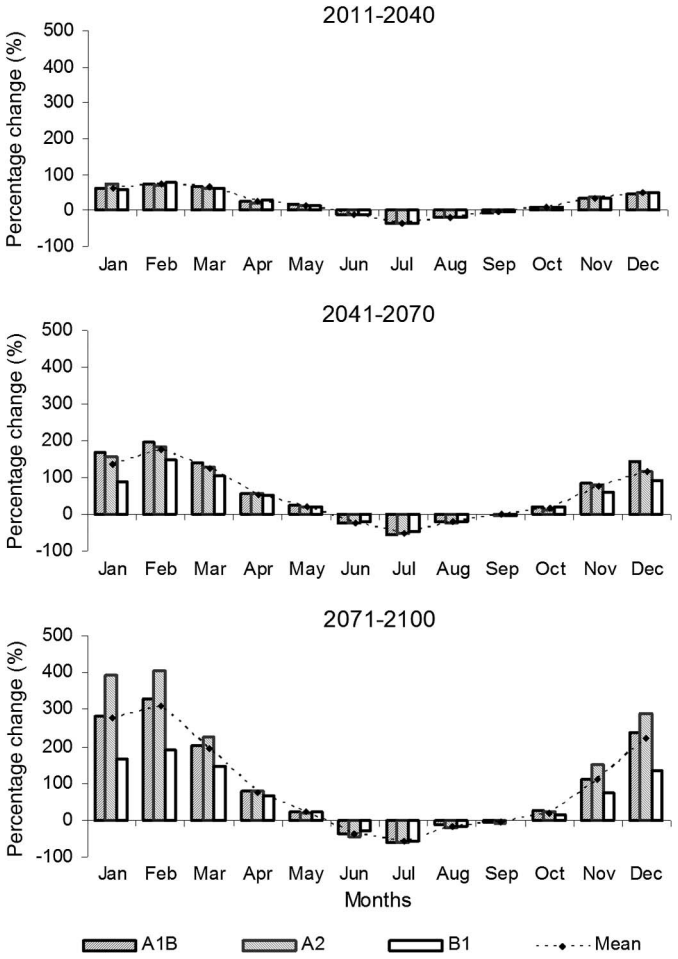

Fig. 10. Percentage change of monthly streamflows for emission scenarios A1B, A2, and B1, for each 30-year time period with respect to baseline period (1971–2100); the mean in the plot represents an average of monthly changes observed for all scenarios

Conclusions

The hydroclimatic modeling approach as presented in this paper can successfully incorporate higher-resolution climate data (projections) in a process-based hydrological model for streamflow forecasting. This hydroclimatic modeling approach has simulated the ensemble of hydrologic changes on the basis of 112 downscaled climate projections from 16 GCMs and 3 emission scenarios. The coupling of higher-resolution BCSD climate data and a hydrologic model has made it possible to evaluate the range of possible hydrologic changes and perform an intermodel, interscenario comparison. However, the ensemble of results represents the mean (central) value such that all climate projections are considered equally likely during this analysis. This is the most comprehensive study to date for the North Platte River watershed that took into account the multimodel, multiscenario downscaled data recently available for climate change studies.

The ensemble averages of climate data for all scenarios showed increasing temperature and precipitation patterns over the course of this century for the North Platte River watershed. Streamflow projections are developed on the basis of forecasted multimodel, multiscenario climate projections for the watershed. The simulated annual streamflows based on different emission scenarios and future time periods (2011–2040, 2041–2070, and 2071–2100) vary from −20 to 62% with respect to 1971–2000. Although the

J. Hydrol. Eng. 2012.17:1071-1083.

simulated streamflows showed larger variation (both increasing and decreasing) under changing climatic conditions at different future time periods, the ensemble of simulated streamflow projections resulted in increased annual streamflow (on average 5.8%) for this region by 2100. The median change in streamflow based on ensemble streamflow projections was higher during 2071–2100 with respect to 1971–2000. The GCM simulating the maximum change (positive or negative) in streamflow varied depending on the scenario. However, for probable maximum and minimum streamflows (90th and 10th percentiles) by 2100, the ensemble of simulated streamflows showed the same range of variation between the scenarios. An increase in streamflow was predicted for cold seasons and a greater reduction during dry seasons; a maximum increase or decrease was observed at the end of this century. Managing water in this basin under anthropogenic climate conditions will be a challenging job when this reduction in streamflow during summer periods coincides with increasing water demand.

To address current issues of water demand and water-rights conflicts in Wyoming, a Wyoming Weather Modification Pilot Program has been in operation to increase snowpack and runoff in major river basins including the North Platte River watershed. Modeled streamflow responses under various WM scenarios over this watershed were carried out in a separate paper. This study, which assessed the potential impacts of climate change on future water resources, could be helpful in managing available future water resources more effectively while observing the results of operational WM programs over the basin. The developed streamflow projections and the range of streamflows from this analysis can be utilized by decision makers in designing additional water management measures to meet the diverse water demands and minimize the stress on available water resources over the basin under future climate change conditions.

Acknowledgments

This research is supported through the Wyoming Weather Modification Pilot Project, State of Wyoming, Wyoming Water Development Office (WWDO). The research at the University of Nevada, Las Vegas is supported by Grants NSF EPS-0814372, NOAA NA070AR4310228, DOE DE-FG02-08ER64709, and DOE DE-EE-0000716. The research at the University of Tennessee is supported by NSF AGS-1003393.

The authors would like to acknowledge the modeling groups, Program for Climate Model Diagnosis and Inter-comparison (PCMDI) and WCRP's Working Group on Coupled Modeling (WGCM), for their roles in making available the WCRP CMIP3 multimodel dataset through the "Bias Corrected and Downscaled WCRP CMIP3 Climate Projections" archive at http://gdo-dcp.ucllnl.org/downscaled_cmip3_projections.

The authors would like to acknowledge the Surface Water Modeling Group at the University of Washington for making available the VIC model and the daily gridded meteorological data.

The authors would like to acknowledge Dr. Andy Wood for his personal time and effort in developing the bias-corrected and spatially disaggregated daily climate output from the GCM output that has been utilized in this research.

References

Acharya, A., Piechota, T. C., Stephen, H., and Tootle, G. (2011). "Modeled streamflow response under cloud seeding in the North Platte River watershed." *J. Hydrol.*, 409(1–2), 305–314.

Aizen, V. B., Aizen, E. M., Melack, J. M., and Dozier, J. (1997). "Climatic and hydrologic changes in the Tien Shan, Central Asia." *J. Clim.*, 10(6), 1393–1404.

Barnett, T. P., et al. (2008). "Human-induced changes in the hydrology of the Western United States." *Science*, 319(5866), 1080–1083.

Bates, B. C., Charles, S. P., Summer, N. R., and Fleming, P. M. (1994). "Climate change and its hydrological implications for South Australia." *Trans. Roy. Soc. South Aust.*, 118(1), 35–43.

Beniston, M., et al. (2007). "Future extreme events in European climate: An exploration of regional climate model projections." *Clim. Change*, 81(1), 81–95.

Beyene, T., Lettenmaier, D. P., and Kabat, P. (2010). "Hydrologic impacts of climate change on the Nile River Basin: Implications of the 2007 IPCC scenarios." *Clim. Change*, 100(3–4), 433–461.

Bureau of Reclamation (BOR). (2006). "Drought in the Upper Colorado River Basin." ⟨www.usbr.gov/uc/feature/drought.html⟩ (Jul. 3, 2012).

Cherkauer, K. A., and Lettenmaier, D. P. (2003). "Simulation of spatial variability in snow and frozen soil." *J. Geophys. Res.*, 108, 8858.

Christensen, N. S., and Lettenmaier, D. P. (2007). "A multimodel ensemble approach to assessment of climate change impacts on the hydrology and water resources of the Colorado River Basin." *Hydrol. Earth Syst. Sci.*, 11(4), 1417–1434.

Christenten, N. S., Wood, A. W., Voisin, N., Lettenmaier, D. P., and Palmer, R. N. (2004). "The effects of climate change on the hydrology and water resources of the Colorado River Basin." *Clim. Change*, 62(1–3), 337–363.

Coquard, J., Duffy, P. B., Taylor, K. E., and Iorio, J. P. (2004). "Present and future surface climate in the western U.S.A. as simulated by 15 global climate models." *Clim. Dyn.*, 23(5), 455–472.

Covey, C., et al. (2003). "An overview of results from the coupled model intercomparison project." *Global Planet. Change*, 37(1–2), 103–133.

Dettinger, M. D., and Cayan, D. R. (1995). "Large-scale atmospheric forcing of recent trends toward early snowmelt runoff in California." *J. Clim.*, 8(3), 606–623.

Easterling, W. E., Mearns, L. O., Hays, C. J., and Marx, D. (2001). "Comparison of agricultural impacts of climate change calculated from high and low resolution climate change scenarios. II: Accounting for adaptation and CO_2 direct effects." *Clim. Change*, 51(2), 173–197.

Fowler, H. J., and Ekström, M. (2009). "Multi-model ensemble estimates of climate change impacts on UK seasonal precipitation extremes." *Int. J. Climatol.*, 29(3), 385–416.

Hamlet, A. F., Mote, P. W., Clark, M. P., and Lettenmaier, D. P. (2005). "Effects of temperature and precipitation variability on snowpack trends in the western United States." *J. Clim.*, 18(21), 4545–4561.

Hayhoe, K., Cayan, D., Field, C. B., Frumhoff, P. C., Maurer, E. P., and Verville, J. H. (2004). "Emission pathways, climate change, and impacts on California." *Proc. Natl. Acad. Sci. USA*, 101(34), 12422–12427.

Held, I. M., and Sodden, B. J. (2006). "Robust responses of the hydrological cycle to global warming." *J. Clim.*, 19(21), 5686–5699.

Hidalgo, H. G., Das, T., Dettinger, M. D., Cayan, D. R., Pierce, D. W., and Nozawa, T. (2009). "Detection and attribution of streamflow timing changes to climate change in the western United States." *J. Clim.*, 22(13), 3838–3855.

Hunter, S. M. (2007). "Optimizing cloud seeding for water and energy in California." *A pierfinal project report prepared for California Energy Commission*, *CEC-500-2007-008* U.S. Bureau of Reclamation.

Intergovernmental Panel on Climate Change (IPCC). (2007a). "Climate change 2007: The physical science basis." *Contribution of Working Group I to the Fourth Assessment Report of the Intergovernmental Panel on Climate Change*, Cambridge Univ. Press, Cambridge.

Intergovernmental Panel on Climate Change (IPCC). (2007b). "Climate change 2007: Synthesis report." *Summary for Policymakers, Fourth Assessment Report of the Intergovernmental Panel on Climate Change*, Cambridge University Press, Cambridge.

Jian, W., and Shuo, L. (2006). "Effect of climate change on snowmelt runoffs in mountainous regions of inland rivers in Northwestern China." *Sci. China*, 49(8), 881–888.

Jung, W., II, and Chang, H. (2011). "Assessment of future runoff trends under multiple climate change scenarios in the Willamette River Basin, Oregon, USA." *Hydrol. Processes*, 25(2), 258–277.

Kang, B., and Ramírez, J. A. (2007). "Response of streamflow to weather variability under climate change in the Colorado Rockies." *J. Hydrol. Eng.*, 12(1), 63–72.
Kim, J., Kim, T. K., Arritt, R. W., and Miller, N. L. (2002). "Impacts of increased atmospheric CO_2 onthe hydroclimate of the western United States." *J. Clim.*, 15(14), 1926–1942.
Knowles, N., Dettinger, M. D., and Cayan, D. R. (2006). "Trends in snowfall versus rainfall in the western United States." *J. Clim.*, 19(18), 4545–4559.
Lambert, S. J., and Boer, G. J. (2001). "CMIP1 evaluation and intercomparison of coupled climate." *Clim. Dyn.*, 17(2–3), 83–106.
Leung, L. R., and Ghan, S. J. (1999). "Pacific Northwest climate sensitivity simulated by a regional climate model driven by a GCM. II: 2 ·CO_2 simulations." *J. Clim.*, 12(7), 2031–2053.
Leung, R. B., Qian, Y., Bian, X., Washington, W. M., Han, J., and Roads, J. O. (2004). "Mid-century ensemble regional climate change scenarios for the western United States." *Clim. Change*, 62(1–3), 75–113.
Liang, X., Lettenmaier, D. P., Wood, E. F., and Burges, S. J. (1994). "A simple hydrologically based model of land surface water and energy fluxes for general circulation models." *J. Geophys. Res.*, 99(14), 415–428.
Lohmann, D., Nolte-Holube, R., and Raschke, E. (1996). "A large scale horizontal routing model to be coupled to land surface parameterization schemes." *Tellus*, 48A, 708–721.
Loukas, A., Vasiliades, L., and Dalezios, N. R. (2002). "Potential climate change impacts on flood producing mechanisms in southern British Columbia, Canada using the CGCMA1 simulation results." *J. Hydrol.*, 259(1–4), 163–188.
Maurer, E. P. (2007). "Uncertainty in hydrologic impacts of climate change in the Sierra Nevada, California, under two emissions scenarios." *Clim. Change*, 82(3–4), 309–325.
Maurer, E. P., Brekke, L., Pruitt, T., and Duffy, P. B. (2007). "Fine-resolution climate projections enhance regional climate change impact studies." *EOS Trans. Am. Geophys. Union*, 88(47), 504.
Maurer, E. P., Hidalgo, H. G., Das, T., Dettinger, M. D., and Cayan, D. R. (2010). "Assessing climate change impacts on daily streamflow in California: The utility of daily large scale climate data." *Hydrol. Earth Syst. Sci. Discuss.*, 7(1), 1209–1249.
Maurer, E. P., Wood, A. W., Adam, J. C., Lettenmaier, D. P., and Nijssen, B. (2002). "A long term hydrologically based dataset of land surface fluxes and states for the conterminous United States." *J. Clim.*, 15(22), 3237–3251.
McGuffie, K., Sellers, A. H., Holbrook, N., Kothavala, Z., Balachova, O., and Hoekstra, J. (1999). "Assessing simulations of daily temperature and precipitation variability with global climate models for present and enhanced greenhouse climates." *Int. J. Climatol.*, 19(1), 1–26.
Miller, W. P., Piechota, T. C., Gangopadhyay, S., and Pruitt, T. (2010). "Development of streamflow projections under changing climate conditions over Colorado River Basins headwaters." *Hydrol. Earth Syst. Sci. Discuss.*, 7(4), 5577–5619.
Milly, P. C. D., et al. (2008). "Stationarity is dead: Whither water management?" *Science*, 319, 573–574.
Milly, P. C. D., Dunne, K. A., and Vecchia, A. V. (2005). "Global pattern of trends in streamflow and water availability in a changing climate." *Nature*, 438(7066), 347–350.
Mote, P. W., Hamlet, A. F., Clark, M. P., and Lettenmaier, D. P. (2005). "Declining mountain snowpack in western North America." *Bull. Am. Meteorol. Soc.*, 86(1), 39–49.
National Aeronautics and Space Administration (NASA). (2008). ⟨http://geology.com/nasa/human-linked-climate-change.shtml⟩ (Apr. 2008).
National Center for Atmospheric Research (NCAR). (2011). "Wyoming weather modification pilot project." ⟨http://www.ral.ucar.edu/projects/wyoming/⟩ (Mar. 2011).
Nebraska v. Wyoming. (1945). 108 (Original), 325 U.S. 589, 665 (U.S. Supreme Court 1945).
Nebraska v. Wyoming and Colorado. (2001). 534 U.S. 40 (U.S. Supreme Court 2001).
Nijssen, B., Donnell, G. M., Hamlet, A. F., and Lettenmaier, D. P. (2001). "Hydrologic sensitivity of global rivers to climate change." *Clim. Change*, 50(1/2), 143–175.
Ojima, D., Garcia, L., Elgaali, E., Miller, K., Kittel, T. G. F., and Lackett, J. (1999). "Potential climate change impacts on water resources in the Great Plains." *J. Am. Water Resour. Assoc.*, 35(6), 1443–1454.
Payne, J. T., Wood, A. W., Hamlet, A. F., Palmer, R. N., and Lettenmaier, D. P. (2004). "Mitigating the effects of climate change on the water resources of the Columbia River Basin." *Clim. Change*, 62, 233–256.
Peterson, A. T. (2003). "Projected climate change effects on rocky mountain and great plains birds." *Global Change Biol.*, 9(5), 647–665.
Pierce, D. W., Barnett, T. P., Hidalgo, H. G., Das, T., Bonfils, C., and Nozawa, T. (2008). "Attribution of declining western U.S. snowpack to human effects." *J. Clim.*, 21(23), 6425–6443.
Raff, D. A., Pruitt, T., and Brekke, L. D. (2009). "A framework for assessing flood frequency based on climate projection information." *Hydrol. Earth Syst. Sci. Discuss.*, 13, 2119–2136.
Roos, M. (1991). "A trend of decreasing snowmelt runoff in Northern California." *Proc., 59th Western Snow Conf.*, Juneau, AK, 29–36.
Shinker, J., Shuman, B., Minckley, T., and Henderson, A. (2010). "Climatic shifts in the availability of contested waters: A long-term perspective from the headwaters of the North Platte River." *Ann. Assoc. Am. Geogr.*, 100(4), 866–879.
Shrestha, R. R., Berland, A. J., Schnorbus, M. A., and Werner, A. T. (2011). "Climate change impacts on hydroclimatic regimes in the Peace and Columbia watersheds, British Columbia, Canada." *A Synthesis Project Final Report*, Pacific Climate Impacts Consortium, Univ. of Victoria, Victoria, BC, 37.
Stephens, M. A. (1970). "Use of the Kolmogorov–Smirnov, Cramer–Von Mises and related statistics without extensive tables." *J. Roy. Stat. Soc.*, 32B, 115–122.
Stewart, I. T., Cayan, D. R., and Dettinger, M. D. (2005). "Changes toward earlier streamflow timing across western North America." *J. Clim.*, 18(8), 1136–1155.
Timilsena, J., Piechota, T. C., Hidalgo, H., and Tootle, G. (2007). "Five hundred years of hydrological drought in the Upper Colorado River Basin." *J. Am. Water Resour. Assoc.*, 43(3), 798–812.
U.S. Dept. of the Interior (DOI). (2003). "Water 2025: Preventing crises and conflict in the West." Bureau of Reclamation ⟨http://www.usbr.gov/WaterSMART⟩ (Jul. 3, 2012).
U.S. Global Change Research Program. (2009). "Great Plains climate change." ⟨http://geology.com/climate-change/great-plains/⟩ (May 2009).
University of Washington. (2012). "Land Surface Hydrology Research Group." ⟨http://www.hydro.washington.edu/SurfaceWaterGroup/data.php⟩ (Jul. 3, 2012).
USGS. (2004). "Climatic fluctuations, drought, and flow in the Colorado River Basin." *USGS Fact Sheet 2004–3062*, ⟨http://pubs.usgs.gov/fs/2004/3062⟩ (Aug. 2004).
Vicuna, S., Maurer, E. P., Joyce, B., Dracup, J. A., and Purkey, D. (2007). "The sensitivity of California water resources to climate change scenarios." *J. Am. Water Resour. Assoc.*, 43(2), 482–498.
Villarini, G., Serinaldi, F., Smith, J. A., and Krajewski, W. F. (2009). "On the stationarity of annual flood peaks in the continental United States during the 20th century." *Water Resour. Res.*, 45(8), W08417.
Wang, J., Hong, Y., Gourley, J., Adhikari, P., Li, L., and Su, F. (2009). "Quantitative assessment of climate change and human impacts on long term hydrologic response." *Int. J. Climatol.*, 30, 2130–2137.
Weiss, A., Hays, C. J., and Won, J. (2003). "Assessing winter wheat responses to climate change scenarios: A simulation study in the US Great Plains." *Clim. Change*, 58(1/2), 119–147.
Wood, A. W., Leung, L. R., Sridhar, V., and Lettenmaier, D. P. (2004). "Hydrologic implications of dynamical and statistical approaches to downscaling climate model outputs." *Clim. Change*, 62(1–3), 189–216.
Woodhouse, C. A., Gray, S. T., and Meko, D. M. (2006). "Updated streamflow reconstructions for the Upper Colorado River Basin." *Water Resour. Res.*, 42(5), W05415.
Wyoming v. Colorado. (1922). 259 U.S. 419 (U.S. Supreme Court 1922, ammended in 1957).
Wyoming Weather Development Commission (WWDC). (2005). "Wyoming level II weather modification feasibility study." Feasibility Study Rep. Prepared for Wyoming Water Development Commission.

J. Hydrol. Eng. 2012.17:1071-1083.